



ELSEVIER

Available online at www.sciencedirect.com

ScienceDirect

www.elsevier.com/locate/jes

JES
JOURNAL OF
ENVIRONMENTAL
SCIENCES
www.jesc.ac.cn

Role of hydrogen bond capacity of solvents in reactions of amines with CO₂: A computational study

Q4

Q3

Tingting Wang¹, Hong-Bin Xie^{1,*}, Zhiquan Song¹, Junfeng Niu²,
De-Li Chen³, Deming Xia¹, Jingwen Chen¹

¹ Key Laboratory of Industrial Ecology and Environmental Engineering (Ministry of Education), School of Environmental Science and Technology, Dalian University of Technology, Dalian 116024, China

² Research Center for Eco-environmental Engineering, Dongguan University of Technology, Dongguan 523808, China

³ Key Laboratory of the Ministry of Education for Advanced Catalysis Materials, Zhejiang Normal University, Jinhua 321004, China

ARTICLE INFO

Article history:

Received 15 September 2019

Received in revised form

15 January 2020

Accepted 21 January 2020

Available online xxx

Keywords:

CO₂ capture

Amine solutions

Solvent effect

Hydrogen bond capacity

Quantum and molecular mechanics

(QM/MM) simulation

Ab initio molecular dynamic (AIMD) simulation

ABSTRACT

Various computational methods were employed to investigate the zwitterion formation, a critical step for the reaction of monoethanolamine with CO₂, in five solvents (water, monoethanolamine, propylamine, methanol and chloroform) to probe the effect of hydrogen bond capacity of solvents on the reaction of amine with CO₂ occurring in the amine-based CO₂ capture process. The results indicate that the zwitterion can be formed in all considered solvents except chloroform. For two pairs of solvents (methanol and monoethanolamine, propylamine and chloroform) with similar dielectric constant but different hydrogen bond capacity, the solvents with higher hydrogen bond capacity (monoethanolamine and propylamine) facilitate the zwitterion formation. More importantly, kinetics parameters such as activation free energy for the zwitterion formation are more relevant to the hydrogen bond capacity than to dielectric constant of the considered solvents, clarifying the hydrogen bond capacity could be more important than dielectric constant in determining the kinetics of monoethanolamine with CO₂.

© 2020 The Research Center for Eco-Environmental Sciences, Chinese Academy of Sciences. Published by Elsevier B.V.

Introduction

Among numerous targets for reducing atmospheric CO₂ emissions, the coal-fired power generation sector has been considered as the most possible one (Alcalde et al., 2018;

Anwar et al., 2018; Schreiber et al., 2009). Currently, post-combustion CO₂ capture (PCC) technology, employing amine solutions to perform reversible capture CO₂, is identified as the most promising technology for CO₂ capture from flue gas of the coal-fired power generation sector (Kenarsari et al.,

* Corresponding author.

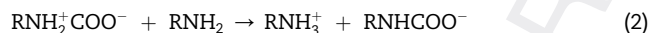
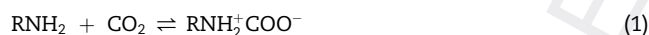
E-mail address: hbxie@dlut.edu.cn (H.-B. Xie).

<https://doi.org/10.1016/j.jes.2020.01.019>

1001-0742/© 2020 The Research Center for Eco-Environmental Sciences, Chinese Academy of Sciences. Published by Elsevier B.V.

2013; Liang et al., 2015; Mondal et al., 2012; Rochelle, 2009; Yang et al., 2017; Yu et al., 2012). Monoethanolamine (MEA) aqueous solution (30 wt.%) was extensively studied as a benchmark solvent for PCC, because of its fast absorption rate and high absorption capability (Abu-Zahra et al., 2007; Chakma et al., 1995; Yang et al., 2017). However, due to its high-energy requirement for the solvent regeneration, the large-scale application of aqueous MEA solution is still impeded (Bhown and Freeman, 2011; Espinal et al., 2013; Mondal et al., 2012; Yang et al., 2016). Therefore, in recent decades, great efforts have been made to optimally design novel amine-based solutions or materials with better performance (Budzianowski, 2015; Darunte et al., 2016; Lu et al., 2017).

An effort to optimize and design novel amine-based solutions or materials is to replace water solvent with an organic solvent or graft amine into solid materials to decrease energy cost in the process of the solvent regeneration (Darunte et al., 2016; Heldebrant et al., 2017; Yu et al., 2017). Some studies have shown that the chemical reaction process for amine capture CO₂ is changed when the surrounding environment of amines is changed (Garcia et al., 2018; Versteeg et al., 2007; Yuan et al., 2019). For instance, in some amine grafted solid materials, primary amine reacting with CO₂ prefers to form carbamic acid rather than carbamate, which is the main product in aqueous amine solutions (Afonso et al., 2019; Flaig et al., 2017). In principle, the change in the chemical process of amine with CO₂ affects the absorption performance for amine capture CO₂. Therefore, it is desirable to investigate the effect of the surrounding environment of amine on chemical process of amine capture CO₂ to optimally design novel amine-based solutions or materials.



Typically, unhindered primary amine like MEA reacts with CO₂ in aqueous solutions via a two-step zwitterion reaction mechanism (Eqs. (1)-(2)) with the first step as the rate-determining one (Caplow, 1968; Danckwerts, 1979; Guido et al., 2013; Han et al., 2013; Han et al., 2011; Hwang et al., 2015; Ma et al., 2014; Nakai et al., 2016; Sumon et al., 2014; Xie et al., 2010). An experimental study by Sada et al. proposed that the overall second-order reaction rate constants of ethylenediamine with CO₂ in methanol, ethanol and water were proportional to the dielectric constant of the solvent (Sada et al., 1985). However, the relationship between the reaction rate constants and dielectric constant of the solvents can be varied when the reactions of other amines with CO₂ were considered (Ali, 2005; Alvarez-Fuster et al., 1980; Hartono et al., 2009; Henni et al., 2008; Kadiwala et al., 2012; Versteeg et al., 1988; Zhong et al., 2016). Recently, the computational studies with implicit solvent model found the dielectric constant of solvent significantly affects the reaction rate of MEA with CO₂ (Yamada, 2016; Zhang et al., 2018). It deserves mentioning that the implicit solvent model can not well describe the short-range interaction such as hydrogen bonds (Marenich et al., 2009). Based on these findings, it could be concluded that not only the dielectric constant of the solvent

but also other characters of solvents can affect chemical reactions of amine with CO₂. In principle, the studied solvents such as water and alcohol could form hydrogen bonds with amines and CO₂ (Sada et al., 1985). The hydrogen bonds as a short-range interaction could also affect chemical reaction process (Liu et al., 2018; Tan et al., 2018). The recent study indeed found that hydrogen bonds can affect the stability of the transition state for amine reacting with CO₂ in aqueous amine solution (Stowe et al., 2017). Therefore, the hydrogen bond capacity of solvents, as an index for forming hydrogen bonds with fixed solute, could affect the chemical process of amine with CO₂. However, currently, there is no systematic study on how the hydrogen bond capacity of solvent affects chemical process of amine with CO₂, together with dielectric constant of the solvent.

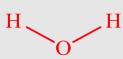
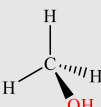
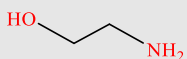
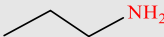
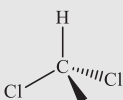
In this study, we investigated the effect of hydrogen bond capacity of solvents on the chemical process of the amine with CO₂ by comparing the chemical processes in solvents with various dielectric constant and hydrogen bond capacity. The zwitterion formation step, a rate-determining one for the reaction of MEA with CO₂ in aqueous solution (Eqs. (1)-(2)), was selected as the target chemical process (Xie et al., 2010). Water, MEA, propylamine (PA), methanol (MA) and chloroform (CHCl₃) were selected as solvents (Table 1). Water, amine and alcohol were commonly studied solvents for CO₂ capture (Budzianowski, 2015; da Silva et al., 2007; Heldebrant et al., 2017; Versteeg et al., 2007). The motivation for selecting CHCl₃ is that it has a similar dielectric constant with PA, however, no ability for forming hydrogen bond with solutes, different from PA. In this way, the role of hydrogen bond capacity can be clearly presented. The employed tool is a combined method of the mixed quantum and molecular mechanics (QM/MM) with *ab initio* molecular dynamic (AIMD). The results will be of significance for the optimal design of novel amine solutions for PCC.

1. Materials and methods

1.1. Potential of mean force calculations

Here, the QM/MM simulations (Hu et al., 2008; Senn et al., 2009) with the umbrella-sampling method (Torrie et al., 1977) were carried out using Amber 12 program to identify the activation free energy for the zwitterion formation step from the reaction of MEA with CO₂ in various solvents. The semi-empirical method PM3-PDDG (parameterized model 3 improved by pairwise distance directed Gaussian function) (Repasky et al., 2002; Walker et al., 2008) was selected as the QM method for all studied systems. Our previous study found the potential for CO₂ attacking N-atom of MEA to form zwitterion at PM3-PDDG level is qualitatively consistent with one at B3LYP/6-31+G(d,p) (the Becke's three-parameter exchange (B3)+Lee-Yang-Parr (LYP) correlation functional) level although the PM3-PDDG slightly underestimates the stability of zwitterion compared with B3LYP/6-31+G(d,p) method (Xie et al., 2014, 2010). Therefore, it is expected that PM3-PDDG/MM method can qualitatively predict the difference in activation free energy and stability of zwitterion for the zwitterion formation step in various solvents. In addition, some critical

Table 1 – Details of solvents in this work.

Solvent	Dielectric constant (ϵ_r)	Molecular Structure
Water	80.1	
Methanol	33.0	
Monoethanolamine	31.9	
Propylamine	5.1	
Chloroform	4.8	

Dielectric constants of all solvents are obtained at about 20°C (Haynes et al., 2016–2017).

results are further confirmed by QM/MM simulation with B3LYP/6-31+G(d,p) as QM method within Gaussian 09 package (Frisch et al., 2009) and *ab initio* molecular dynamics (AIMD) simulations.

The QM/MM simulation systems were built by immersing one MEA and one CO₂ in various solvents with periodic boundary conditions. 2238 water molecules, 1587 MEA molecules, 1584 CHCl₃ molecules, 1586 PA molecules and 1159 MA molecules were involved in their respective simulation systems (Appendix A Fig. S3). The QM subsystem consists of CO₂ and MEA for all studied systems, while all solvent molecules were treated with molecular mechanics. The TIP3P (transferable intermolecular potential with 3 points) model (Jorgensen et al., 1983; Wang et al., 2004; Zielkiewicz, 2005) for water and general Amber force field for MEA, PA, CHCl₃ and MA were employed. Computational densities by adopted force field parameters agree well with corresponding values from experiments for pure solvents (Appendix A Table S1), indicating the reliability of the adopted force field for solvents. For the PM3-PDDG/MM simulation, it was carried out in two successive steps. Each system was equilibrated in NPT (a fixed number of atoms *N*, pressure *P*, and temperature *T*) ensemble for 200–300 psec (Appendix A Fig. S2), followed by 1 nsec NVT

(a fixed number of atoms *N*, volume *V*, and temperature *T*) ensemble production simulation with the umbrella-sampling method for each window. The configuration of last step in 1 nsec simulation with PM3-PDDG/MM potential was selected as initial one for 50 psec NVT ensemble simulation with B3LYP/6-31+G(d,p)/MM potential. In all QM/MM simulations, the time step was 1 fsec and Newton's equations of motion were integrated with the Beeman algorithm. Cutoff (10 Å) was employed for both electrostatic and all non-bonded interactions. The long-range electrostatic energy was evaluated using the particle-mesh Ewald summation (Cerutti et al., 2010). The trajectory was saved every 1000 fsec in simulation with PM3-PDDG/MM potential for further hydrogen bond capacity analysis.

The distance between the C atom of CO₂ and the N atom of MEA was chosen as the reaction coordinate. Thirty-six NVT-ensemble simulation windows were placed along the reaction coordinate from 5.0 to 1.5 Å and per window was run with harmonic-restraint potentials imposed on the reaction coordinate (*x*) between the N atom of MEA and C atom of CO₂.

$$V(x) = k(x - x_0)^2 \quad (1)$$

where *V*(*x*) is harmonic-restraint potential, the force constant is *k* = 20 kcal/(mol·Å²) and the “equilibrium” reaction coordinate (*x*₀) for a given window is set every 0.1 Å from 5.0 to 1.5 Å. The points from the PM3-PDDG/MM simulations were saved every 0.1 psec and a total number of 10,000 points were collected for each window. The points from the B3LYP/6-31+G(d,p)/MM simulations were saved every 20 fsec and a total number of 2500 points were collected for each window. To determine the potential of mean force (PMF) for all studied systems, we processed the data from all the windows using the weighted histogram analysis method (WHAM) (Kumar et al., 1992). The bin dimension and temperature applied in the WHAM calculation of the PMF was 0.05 Å and 298 K, respectively.

1.2. Hydrogen bond capacity analysis

Currently, there is no appropriate empirical parameter to describe the hydrogen bond capacity. We noted that Seiler et al. tried to use the difference between the 1-octanol-water partition coefficient and the cyclohexane-water partition coefficient as a measure of the hydrogen bonding capacity (Seiler et al., 1974). However, el Tayar et al. thought it mainly accounts for the hydrogen bond donor capacity, but not total hydrogen bonding capacity of solvent (el Tayar et al., 1991). In fact, it is understandable that the hydrogen bond capacity of solvent is hard to be quantitatively described by a static parameter since it also depends on the characters of specific solutes. Instead, the hydrogen bond occurrence probability was used to present hydrogen bond capacity of solvents here, a similar strategy used in previous study (el Tayar et al., 1993). The Ptraj module in AMBER 12 was utilized to probe hydrogen bond occurrence probability between MEA + CO₂ solute and solvents in the simulation. The hydrogen bond is defined by the geometric criteria, i.e., the distance between *X* and *Y* (*X* = O, N of solvent and *Y* = O, N of solute) shorter than 3.5 Å and the angle *X*–H...*Y* or *Y*–H ... *X* within 150–180°

(Chowdhuri et al., 2002). The hydrogen bond occurrence probability (P_{HB}) can be calculated by the following formula:

$$P_{HB} = \frac{N}{7000} \times 100\% \quad (2)$$

where N is the number forming the hydrogen bonds, 7000 is the total number of hydrogen bonds when all possible hydrogen bond donors and acceptors of MEA and CO_2 form hydrogen bonds with solvents. Computational details for the total number of all hydrogen bonds are shown in [Appendix A Supplementary data](#).

1.3. Ab initio molecular dynamics simulations

To further confirm the results obtained from QM/MM simulation, AIMD simulations were performed to assess the stability of zwitterion in PA and CHCl_3 solvent. For PA solvent system, the cubic simulation box consists of 1 zwitterion molecule and 21 PA molecules with a cell parameter of 15.211 Å. For the CHCl_3 solvent system, the cubic simulation box consists of 1 zwitterion and 35 CHCl_3 molecules with a cell parameter of 16.800 Å ([Appendix A Fig. S4](#)). Initial configurations in AIMD simulations were obtained by cutting off redundant solvent molecules from PM3-PDDG/MM simulations for windows with N–C equilibrium distance close to identified (or assumed) N–C distance of zwitterion. All AIMD simulations were performed in NVT ensemble for 10 psec by the Vienna *ab initio* simulation package (VASP, version 5.4.1) ([Hafner, 2008](#)). The time step is 1 fsec. The simulation temperature was set as 298 K. Periodic density functional theory (DFT) with the PW91 exchange-correlation functional was used for electronic structure calculation ([Perdew et al., 1996](#)). The projector augmented wave (PAW) method with a potpaw GGA-wave basis set was employed to describe the interaction between the core and valence electrons ([Blochl et al., 2003](#)). Given the simulation system is asymmetric, only the gamma point was sampled for Brillouin zone integration.

2. Results and discussion

2.1. Potential of mean force calculations with PM3-PDDG/MM potential

The PMF curves, obtained at PM3-PDDG/MM level and 298 K, for C-atom of CO_2 approaching N-atom of MEA from 5.0 to 1.5 Å in five selected solvents were presented in [Fig. 1](#). It can be observed that, except CHCl_3 , the free energy increases with the decrease of C–N distance from 5.0 Å to about 1.8–2.0 Å in all solvents, where the free energy reaches a maximum. The maximum corresponds to the transition state structure for the zwitterion formation reaction. Then, the free energy decreases from the transition state to a local minimum with the C–N distances about 1.6 Å. The local minimum corresponds to the zwitterion intermediate MEA^+COO^- . Exactly, the C–N distances of transition states in water, MA, MEA, PA, are 2.02, 1.84, 2.02 and 1.93 Å, and corresponding distances of zwitterion are 1.63, 1.66, 1.63, 1.63 Å, respectively. The snapshots of transition states and zwitterion in different solvent are presented in [Appendix A Fig. S5](#). In CHCl_3 solvent, the free

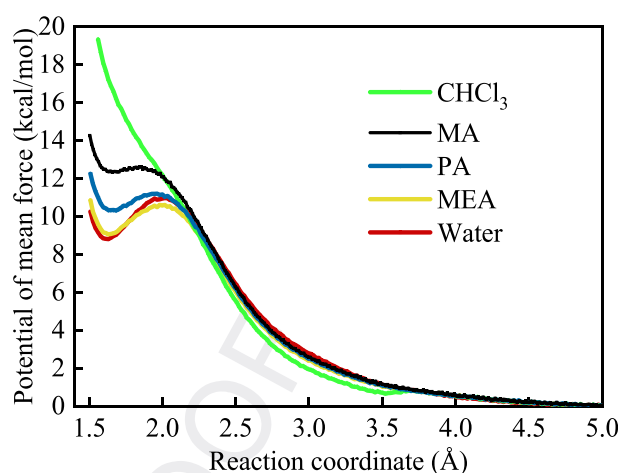


Fig. 1 – Potential of mean force plot for C-atom of CO_2 approaching N-atom of monoethanolamine (MEA) in five different solvents obtained at PM3-PDDG/MM level of theory. The distance between the C atom of CO_2 and the N atom of MEA is taken as the reaction coordinate. PA: propylamine; MA: methanol; PM3-PDDG: parameterized model 3 improved by pairwise distance directed Gaussian function; MM: molecular mechanics.

energy continuously increases with the decrease of C–N distance from 5.0 to 1.5 Å, indicating that the transition state and the zwitterion intermediate are not formed in CHCl_3 solvent, and therefore no zwitterion formation reaction occurs between MEA and CO_2 in CHCl_3 solvent. Since the dielectric constant of CHCl_3 is similar to that of PA ([Table 1](#)), the key difference between CHCl_3 and PA that could affect the chemical process of MEA with CO_2 is the hydrogen bond capacity (CHCl_3 can not form hydrogen bond with solute, while PA can). Therefore, the different reaction process of CO_2 toward MEA in CHCl_3 and PA solvents indicates that the hydrogen bond capacity of solvent plays a vital role in determining the zwitterion formation from MEA and CO_2 .

The activation free energies (ΔG^\ddagger) for the zwitterion formation predicted by PMF calculation are 11.0, 10.6, 11.2 and 12.6 kcal/mol in water, MEA, PA and MA solvent, respectively. Obviously, ΔG^\ddagger in MA ($\Delta G^\ddagger_{\text{MA}}$) solvent is the highest among all considered solvents and the ΔG^\ddagger in water ($\Delta G^\ddagger_{\text{Water}}$), MEA ($\Delta G^\ddagger_{\text{MEA}}$) and PA ($\Delta G^\ddagger_{\text{PA}}$) are similar. In addition, the free energy difference ($\Delta G_{\text{Z-T}}$) between zwitterion and corresponding transition state, an important parameter affecting the kinetics of reaction of MEA with CO_2 (the greater $\Delta G_{\text{Z-T}}$, the more favorable the formation of zwitterion in kinetics) ([Xie et al., 2010](#)), are 2.2, 1.6, 0.9 and 0.3 kcal/mol in water, MEA, PA, and MA solvent, respectively. $\Delta G_{\text{Z-T}}$ is the highest in water solvent and is the lowest in MA solvent. It deserves mentioning that the dielectric constant of PA is the lowest among all considered solvents, and MA is similar to that of MEA, which both are lower than that of water. Thus, there is no good relationship between $\Delta G^\ddagger/\Delta G_{\text{Z-T}}$ and dielectric constant of solvent, implying dielectric constant of solvent is not the only important parameter to determine reaction kinetics of MEA with CO_2 . Combined with results from the comparison for the chemical process of zwitterion formation from the

reaction of MEA with CO₂ in CHCl₃ and PA solvent, it can be concluded that the hydrogen bond capacity of solvents plays an important role in determining the occurrence or kinetics of the reaction of MEA with CO₂.

2.2. Hydrogen bond occurrence probability analysis

To identify the difference in hydrogen bond occurrence probability between MEA + CO₂ solute with solvent molecules in various solvents, three typical windows with C–N equilibrium distance 5.0 Å and close to identified C–N distance of zwitterion, transition state from PMF simulation were selected as trajectories of reactants, zwitterion and transition state, to do hydrogen bond occurrence probability analysis. Since no hydrogen bond can be formed between MEA + CO₂ solute and CHCl₃ solvent molecules, hydrogen bond occurrence probability between MEA + CO₂ and CHCl₃ is zero. Therefore, hydrogen bond occurrence probability statistics were only performed in water, MA, MEA and PA solvents with Ptraj module in Amber 12. Results of hydrogen bond occurrence probability were shown in Fig. 2 and the detailed statistical data of different types hydrogen bonds are summarized in Appendix A Table S2.

As can be seen in Fig. 2, for each solvent, the hydrogen bond occurrence probability of zwitterion (P_Z), transition state (P_T) and reactant (P_R) follows an order of $P_Z > P_T > P_R$. This indicates that with the decreasing C–N distance in the process of C-atom of CO₂ attacking N-atom of MEA, the interaction between MEA and CO₂ increases the hydrogen bond capacity of MEA + CO₂ solute. The zwitterion formation leads to more hydrogen bond formation between MEA + CO₂ solute and solvents. However, for the same species of MEA + CO₂ system, the hydrogen bond occurrence probability is different in various solvents. The hydrogen bond occurrence probability (P_{water} , P_{MEA} , P_{PA} and P_{MA} in water, MEA, PA and MA) for the same species in various solvents follows $P_{\text{water}} > P_{\text{MEA}} > P_{\text{PA}} > P_{\text{MA}}$, well consistent with the order of ΔG_{Z-T} and little different from the order of stability of transition states (which reverses to the order of ΔG^\ddagger ($\Delta G^\ddagger_{\text{MEA}} < \Delta G^\ddagger_{\text{Water}} < \Delta G^\ddagger_{\text{PA}} < \Delta G^\ddagger_{\text{MA}}$)) with

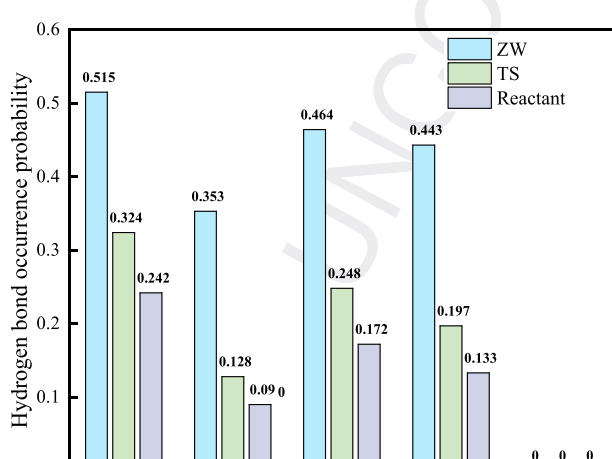


Fig. 2 – Hydrogen bond occurrence probability between MEA + CO₂ solute and five solvents water, MA, MEA, PA and CHCl₃. ZW: zwitterion; TS: transition state.

MEA as an exception in these solvents (detailed relationship between the kinetic parameters (ΔG_{Z-T} and ΔG^\ddagger) and hydrogen bond capacity (P) is presented in Appendix A Fig. S7). Thus, the hydrogen bond capacity of solvent is more relevant to the kinetics of MEA with CO₂ than the dielectric constant of solvent. More importantly, for solvents MEA and MA, which have the similar dielectric constant, the zwitterion formation in MEA solvent with higher hydrogen bond capacity is more favorable than that in MA solvent since the reaction in MEA solvent has higher ΔG_{Z-T} and lower ΔG^\ddagger . Besides, for solvents CHCl₃ and PA, which have a similar dielectric constant and different hydrogen bond capacity, MEA can not react with CO₂ in CHCl₃ solvent, but can in PA solvent. These could indicate that the hydrogen bond capacity of solvents is more important than dielectric constant in determining kinetics of MEA with CO₂. To be best of our knowledge, it is the first time to point the importance of hydrogen bond capacity of solvent in affecting the reaction kinetics of amine with CO₂.

2.3. B3LYP/6-31+G(d,p)/MM and AIMD simulations

Perhaps the most questionable part of the above results is that low-level PM3-PDDG method is used to simulate solute and molecular mechanics method is used to simulate solvent. Here, both PMF with B3LYP/6-31+G(d,p)/MM potential and AIMD simulation were performed to further confirm the important results from PM3-PDDG/MM method. The difference in reaction process of MEA with CO₂ in CHCl₃ and PA solvent clearly present the importance of hydrogen bond capacity of solvent in determining the zwitterion formation from the reaction of MEA with CO₂. Thus, the confirmation simulation is only performed on the reaction of MEA with CO₂ in CHCl₃ and PA solvent to save computational resources. In addition, since the reaction of CO₂ with MEA could not occur in CHCl₃ solvent and could take a very long time to react in PA solvent, AIMD simulations were performed starting from zwitterion intermediate.

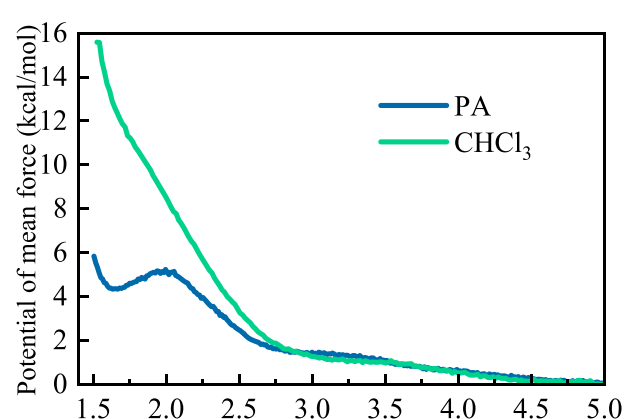


Fig. 3 – Potential of mean force plot for C-atom of CO₂ approaching N-atom of MEA in CHCl₃ and PA solvent obtained at B3LYP/6-31+G(d,p)/MM theory of level. The distance between the C atom of CO₂ and the N atom of MEA is taken as the reaction coordinate. B3LYP: the Becke's three-parameter exchange (B3)+Lee-Yang-Parr (LYP) correlation functional.

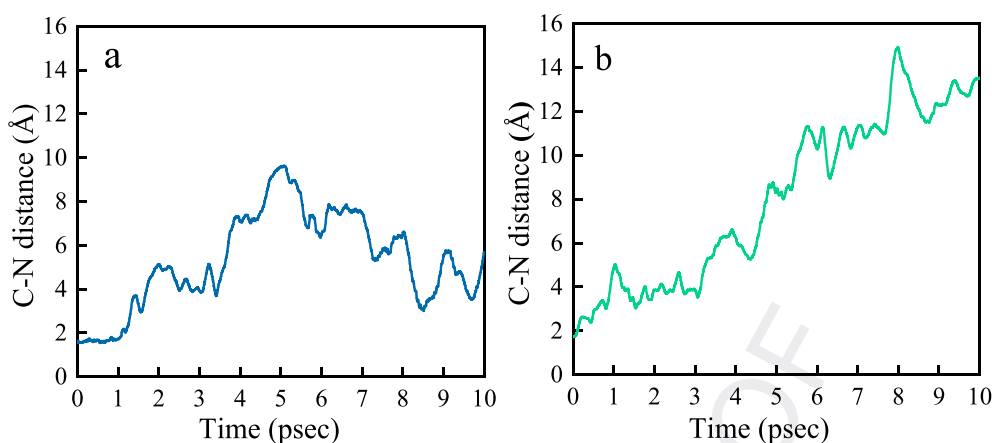


Fig. 4 – Time evolution of the distance between the C atom of CO₂ and N atom of MEA in (a) PA and (b) CHCl₃ solvent during 10 psec *ab initio* molecular dynamic (AIMD) simulation.

The PMF curves, obtained at B3LYP/6-31+G(d,p)/MM level, for C-atom of CO₂ approaching N of MEA from 5.0 to 1.5 Å in PA and CHCl₃ solvents are presented in Fig. 3. As can be seen in Fig. 3, the reaction of MEA with CO₂ to form zwitterion still can occur in PA solvent. ΔG^\ddagger value for the reaction of MEA with CO₂ in PA solvent at B3LYP/6-31+G(d,p)/MM level is lower than that at PM3-PDDG/MM level. However, the reaction still can not occur in CHCl₃ solvent. The difference in the reaction process of MEA with CO₂ in these two solvents, predicted by B3LYP/6-31+G(d,p)/MM level is well consistent with results from PM3-PDDG/MM level. Therefore, although PM3-PDDG/MM potential could not be quantitatively accurate enough, it is still expected it can provide an acceptable qualitative result for the reaction of MEA with CO₂ in various solvents.

The time evolution of the C–N distance between the C atom of CO₂ and N atom of MEA in PA and CHCl₃ solvent during 10 psec AIMD simulation is shown in Fig. 4. In PA solvent (Fig. 4a), the initial C–N distance of zwitterion is 1.64 Å (Appendix A Fig. S4a). The zwitterion keeps stable for the first 1.1 psec and then separates to form CO₂ and MEA. This indirectly indicates that zwitterion can be formed in the PA solvent, however, the lifetime is short. We also try to compare the lifetime from AIMD with that from QM/MM simulation. Based on transition state theory and ΔG^\ddagger from QM/MM simulation, the lifetime of zwitterion in PA was calculated (see details in Appendix A Supplementary data). The calculated lifetime of zwitterion in PA solvent is 0.687 and 0.723 psec with PM3-PDDG/MM and B3LYP/6-31+G(d,p)/MM as the potential in the QM/MM simulation, respectively, well consistent with that (1.1 psec) from AIMD simulation. In addition, we also observed that the zwitterion is not formed again during 10 psec simulation after the decomposition. It could be understandable since ΔG^\ddagger for the reaction of MEA with CO₂ is high, it will take a longer time to make the reaction of MEA with CO₂ occur than the 10 psec simulation time. In CHCl₃ solvent (Fig. 4b), the initial C–N distance of zwitterion is 1.69 Å (Appendix A Fig. S4b). The C–N distance rapidly increased once the simulation was started. Even 1.62 Å was used as the initial C–N distance, the same as in PA solvent, C–N distance still rapidly increased once the simulation was started (Appendix A Fig. S6) in CHCl₃ solvent. This indirectly indicates that the zwitterion can not be formed in the CHCl₃ solvent, consistent

with that from QM/MM simulation. Therefore, the AIMD simulation on the stability of zwitterion further confirms the findings from QM/MM simulation that the reaction of MEA with CO₂ can form the zwitterion in PA solvent, but not in the CHCl₃ solvent.

3. Conclusions

Here, to probe the effect of hydrogen bond capacity of solvents on the reaction of amine with CO₂, various computational methods including PM3-PDDG/MM, B3LYP/6-31+G(d,p)/MM and AIMD were employed to investigate the zwitterion formation from the reaction of MEA with CO₂ in water, MEA, PA, MA and CHCl₃ solvent by explicitly considering the solvent effect. The results indicate that the zwitterion can be formed in water, MEA, PA and MA solvent, but not in CHCl₃ solvent. For two pairs of solvents (MA and MEA, PA and CHCl₃) with similar dielectric constant but different hydrogen bond capacity, the solvents with higher hydrogen bond capacity (MEA and PA) facilitate the zwitterion formation. More importantly, ΔG^\ddagger and ΔG_{Z-T} values, two important parameters determining the kinetics of zwitterion formation, are more relevant to the hydrogen bond capacity than to dielectric constant of the solvents. Therefore, it was concluded that the hydrogen bond capacity of solvent is more important than dielectric constant in determining the kinetics of MEA with CO₂. To be best of our knowledge, it is the first time to point out the importance of hydrogen bond capacity of solvent in affecting the reaction kinetics of amine with CO₂. The hydrogen bond capacity of solvent should be considered in the optimal design of amine for CO₂ capture in the future.

Uncited reference

Sousa et al., 2007.

Conflict of interest

None declared.

Q1 Acknowledgments

This work was supported by the National Natural Science Foundation of China (Nos. 21876024 and 21677028), the Major International (Regional) Joint Research Project (No. 21661142001), the Program for Changjiang Scholars and Innovative Research Team in University (No. IRT_13R05), and the Programme of Introducing Talents of Discipline to Universities (No. B13012) and Supercomputing Center of Dalian University of Technology. Tingting Wang thanks for the supports from her best friend Mr. Zhongyu Guo.

Appendix A. Supplementary data

Supplementary data to this article can be found online at <https://doi.org/10.1016/j.jes.2020.01.019>.

REFERENCES

- Abu-Zahra, M.R.M., Schneiders, L.H.J., Niederer, J.P.M., Feron, P.H.M., Versteeg, G.F., 2007. CO₂ capture from power plants: Part I. A parametric study of the technical performance based on monoethanolamine. *Int. J. Greenh. Gas Con.* 1, 37–46.
- Afonso, R., Sardo, M., Mafra, L., Gomes, J.R.B., 2019. Unravelling the structure of chemisorbed CO₂ species in mesoporous aminosilicas: A critical survey. *Environ. Sci. Technol.* 53, 2758–2767.
- Alcalde, J., Flude, S., Wilkinson, M., Johnson, G., Edlmann, K., Bond, C.E., et al., 2018. Estimating geological CO₂ storage security to deliver on climate mitigation. *Nat. Commun.* 9, 2201.
- Ali, S.H., 2005. Kinetics of the reaction of carbon dioxide with blends of amines in aqueous media using the stopped-flow technique. *Int. J. Chem. Kinet.* 37, 391–405.
- Alvarez-Fuster, C., Midoux, N., Laurent, A., Charpentier, J.C., 1980. Chemical kinetics of the reaction of carbon dioxide with amines in pseudo m-nth order conditions in aqueous and organic Solutions. *Chem. Eng. Sci.* 35, 1717–1723.
- Anwar, M.N., Fayyaz, A., Sohail, N.F., Khokhar, M.F., Baqar, M., Khan, W.D., et al., 2018. CO₂ capture and storage: A way forward for sustainable environment. *J. Environ. Manage.* 226, 131–144.
- Bhown, A.S., Freeman, B.C., 2011. Analysis and status of post-combustion carbon dioxide capture technologies. *Environ. Sci. Technol.* 45, 8624–8632.
- Bloch, P.E., Forst, C.J., Schimpl, J., 2003. Projector augmented wave method: ab initio molecular dynamics with full wave functions. *Bull. Mater. Sci.* 26, 33–41.
- Budzianowski, W.M., 2015. Single solvents, solvent blends, and advanced solvent systems in CO₂ capture by absorption: a review. *Int. J. Global Warm.* 7, 184–225.
- Caplow, M., 1968. Kinetics of carbamate formation and breakdown. *J. Am. Chem. Soc.* 90, 6795–6803.
- Cerutti, D.S., Case, D.A., 2010. Multi-Level Ewald: A hybrid multigrid/fast fourier transform approach to the electrostatic particle-mesh problem. *J. Chem. Theory Comput.* 6, 443–458.
- Chakma, A., Mehrotra, A.K., Nielsen, B., 1995. Comparison of chemical solvents for mitigating CO₂ emissions from coal-fired power-plants. *Heat Recov. Syst. CHP* 15, 231–240.
- Chowdhuri, S., Chandra, A., 2002. Hydrogen bonds in aqueous electrolyte solutions: statistics and dynamics based on both geometric and energetic criteria. *Phys. Rev. E. Stat. Nonlin. Soft Matter. Phys.* 66, 41203.
- da Silva, E.F., Kuznetsova, T., Kvamme, B., Merz, K.M., 2007. Molecular dynamics study of ethanolamine as a pure liquid and in aqueous solution. *J. Phys. Chem. B* 111, 3695–3703.
- Danckwerts, P.V., 1979. The reaction of CO₂ with ethanolamines. *Chem. Eng. Sci.* 34, 443–446.
- Darunte, L.A., Walton, K.S., Sholl, D.S., Jones, C.W., 2016. CO₂ capture via adsorption in amine-functionalized sorbents. *Curr. Opin. Chem. Eng.* 12, 82–90.
- Espinal, L., Poster, D.L., Wong-Ng, W., Allen, A.J., Green, M.L., 2013. Measurement, standards, and data needs for CO₂ capture materials: a critical review. *Environ. Sci. Technol.* 47, 11960–11975.
- Flaig, R.W., Osborn Popp, T.M., Fracaroli, A.M., Kapustin, E.A., Kalmutzki, M.J., Altamimi, R.M., et al., 2017. The chemistry of CO₂ capture in an amine-functionalized metal-organic framework under dry and humid conditions. *J. Am. Chem. Soc.* 139, 12125–12128.
- Frisch, M.J., Trucks, G.W., H.B. S., Scuseria, G.E., Robb, M.A., Cheeseman, J.R., et al., 2009. Gaussian 09; Gaussian, Inc., Wallingford, CT (Control Techniques).
- Garcia, M., Knuutila, H.K., Aronu, U.E., Gu, S., 2018. Influence of substitution of water by organic solvents in amine solutions on absorption of CO₂. *Int. J. Greenh. Gas Con.* 78, 286–305.
- Guido, C.A., Pietrucci, F., Gallet, G.A., Andreoni, W., 2013. The fate of a zwitterion in water from ab initio molecular dynamics: monoethanolamine (MEA)-CO₂. *J. Chem. Theory Comput.* 9, 28–32.
- Hafner, J., 2008. Ab-initio simulations of materials using VASP: density-functional theory and beyond. *J. Comput. Chem.* 29, 2044–2078.
- Han, B., Zhou, C., Wu, J., Tempel, D.J., Cheng, H., 2011. Understanding CO₂ capture mechanisms in aqueous monoethanolamine via first principles simulations. *J. Phys. Chem. Lett.* 2, 522–526.
- Han, B., Sun, Y., Fan, M., Cheng, H., 2013. On the CO₂ capture in water-free monoethanolamine solution: an ab initio molecular dynamics study. *J. Phys. Chem. B* 117, 5971–5977.
- Hartono, A., Svendsen, H.F., 2009. Kinetics reaction of primary and secondary amine group in aqueous solution of diethylenetriamine (DETA) with carbon dioxide. *Energy Proc.* 1, 853–859.
- Haynes, W.M., Lide, D.R., Lide, D.R., 2016–2017. In: CRC (Chemical Rubber Company) handbook of chemistry and physics: a ready-reference book of chemical and physical data, 97th ed. CRC Press.
- Heldebrant, D.J., Koech, P.K., Glezakou, V.A., Rousseau, R., Malhotra, D., Cantu, D.C., 2017. Water-lean solvents for post-combustion CO₂ capture: fundamentals, uncertainties, opportunities, and outlook. *Chem. Rev.* 117, 9594–9624.
- Henni, A., Li, J., Tontiwachwuthikul, P., 2008. Reaction kinetics of CO₂ in aqueous 1-amino-2-propanol, 3-amino-1-propanol, and dimethylmonoethanolamine solutions in the temperature range of 298–313 K using the stopped-flow technique. *Ind. Eng. Chem. Res.* 47, 2213–2220.
- Hu, P., Wang, S., Zhang, Y., 2008. Highly dissociative and concerted mechanism for the nicotinamide cleavage reaction in Sir2Tm enzyme suggested by ab initio QM/MM molecular dynamics simulations. *J. Am. Chem. Soc.* 130, 16721–16728.
- Hwang, G.S., Stowe, H.M., Paek, E., Manogaran, D., 2015. Reaction mechanisms of aqueous monoethanolamine with carbon dioxide: a combined quantum chemical and molecular dynamics study. *Phys. Chem. Chem. Phys.* 17, 831–839.
- Jorgensen, W.L., Chandrasekhar, J., Madura, J.D., 1983. Comparison of simple potential functions for simulating liquid water. *J. Chem. Phys.* 79, 926–935.
- Kadiwala, S., Rayer, A.V., Henni, A., 2012. Kinetics of carbon dioxide (CO₂) with ethylenediamine, 3-amino-1-propanol in methanol and ethanol, and with 1-dimethylamino-2-propanol

- and 3-dimethylamino-1-propanol in water using stopped-flow technique. *Chem. Eng. J.* 179, 262–271.
- Kenarsari, S.D., Yang, D., Jiang, G., Zhang, S., Wang, J., Russell, A.G., et al., 2013. Review of recent advances in carbon dioxide separation and capture. *RSC Adv.* 3, 22739–22773.
- Kumar, S., Rosenberg, J.M., Bouzida, D., Swendsen, R.H., Kollman, P.A., 1992. The weighted histogram analysis method for free-energy calculations on biomolecules. I. The method. *J. Comput. Chem.* 13, 1011–1021.
- Liang, Z., Rongwong, W., Liu, H., Fu, K., Gao, H., Cao, F., et al., 2015. Recent progress and new developments in post-combustion carbon-capture technology with amine based solvents. *Int. J. Greenh. Gas Con.* 40, 26–54.
- Liu, X., Zhang, J., Yang, L., Hase, W.L., 2018. How a solvent molecule affects competing elimination and substitution dynamics. Insight into mechanism evolution with increased solvation. *J. Am. Chem. Soc.* 140, 10995–11005.
- Lu, Z., Godfrey, H.G., da Silva, I., Cheng, Y., Savage, M., Tuna, F., et al., 2017. Modulating supramolecular binding of carbon dioxide in a redox-active porous metal-organic framework. *Nat. Commun.* 8, 14212.
- Ma, C., Pietrucci, F., Andreoni, W., 2014. Capturing CO₂ in monoethanolamine (MEA) aqueous solutions: fingerprints of carbamate formation assessed with first-principles simulations. *J. Phys. Chem. Lett.* 5, 1672–1677.
- Marenich, A.V., Cramer, C.J., Truhlar, D.G., 2009. Universal solvation model based on solute electron density and on a continuum model of the solvent defined by the bulk dielectric constant and atomic surface tensions. *J. Phys. Chem. B* 113, 6378–6396.
- Mondal, M.K., Balsora, H.K., Varshney, P., 2012. Progress and trends in CO₂ capture/separation technologies: A review. *Energy* 46, 431–441.
- Nakai, H., Nishimura, Y., Kaiho, T., Kubota, T., Sato, H., 2016. Contrasting mechanisms for CO₂ absorption and regeneration processes in aqueous amine solutions: insights from density-functional tight-binding molecular dynamics simulations. *Chem. Phys. Lett.* 647, 127–131.
- Perdew, J.P., Burke, K., Ernzerhof, M., 1996. Generalized gradient approximation made simple. *Phys. Rev. Lett.* 77, 3865–3868.
- Repasky, M.P., Chandrasekhar, J., Jorgensen, W.L., 2002. PDDG/PM3 and PDDG/MNDO: improved semiempirical methods. *J. Comput. Chem.* 23, 1601–1622.
- Rochelle, G.T., 2009. Amine scrubbing for CO₂ capture. *Science* 325, 1652–1654.
- Sada, E., Kumazawa, H., Han, Z.Q., 1985. Kinetics of reaction between carbon dioxide and ethylenediamine in nonaqueous solvents. *Chem. Eng. J.* 31, 109–115.
- Schreiber, A., Zapp, P., Kuckshinrichs, W., 2009. Environmental assessment of German electricity generation from coal-fired power plants with amine-based carbon capture. *Int. J. Life Cycle Assess.* 14, 547–559.
- Seiler, P., 1974. Interconversion of lipophilicities from hydrocarbon/water systems into the octanol/water system. *Eur. J. Med. Chem.* 9, 473–479.
- Senn, H.M., Thiel, W., 2009. QM/MM methods for biomolecular systems. *Angew. Chem. Int. Ed. Engl.* 48, 1198–1229.
- Sousa, S.F., Fernandes, P.A., Ramos, M.J., 2007. General performance of density functionals. *J. Phys. Chem. A* 111, 10439–10452.
- Stowe, H.M., Hwang, G.S., 2017. Molecular insights into the enhanced rate of CO₂ absorption to produce bicarbonate in aqueous 2-amino-2-methyl-1-propanol. *Phys. Chem. Chem. Phys.* 19, 32116–32124.
- Sumon, K.Z., Henni, A., East, A.L., 2014. Molecular dynamics simulations of proposed intermediates in the CO₂ + aqueous amine reaction. *J. Phys. Chem. Lett.* 5, 1151–1156.
- Tan, K., Jensen, S., Zuluaga, S., Chapman, E.K., Wang, H., Rahman, R., et al., 2018. Role of hydrogen bonding on transport of coadsorbed gases in metal-organic frameworks materials. *J. Am. Chem. Soc.* 140, 856–859.
- Tayar, N., Tsai, R.S., Testa, B., Carrupt, P.A., Leo, A., 1991. Partitioning of solutes in different solvent systems: the contribution of hydrogen-bonding capacity and polarity. *J. Pharm. Sci.* 80, 590–598.
- Tayar, N., Mark, A.E., Vallat, P., Brunne, R.M., Testa, B., van Gunsteren, W.F., 1993. Solvent-dependent conformation and hydrogen-bonding capacity of cyclosporin A: evidence from partition coefficients and molecular dynamics simulations. *J. Med. Chem.* 36, 3757–3764.
- Torrie, G.M., Valleau, J.P., 1977. Nonphysical sampling distributions in Monte Carlo free-energy estimation: umbrella sampling. *J. Comput. Phys.* 23, 187–199.
- Versteeg, G.F., van Swaaij, W.P.M., 1988. On the kinetics between CO₂ and alkanolamines both in aqueous and non-aqueous solutions—I. Primary and secondary amines. *Chem. Eng. Sci.* 43, 573–585.
- Versteeg, G.F., Van Dijk, L.A.J., Van Swaaij, W.P.M., 2007. On the kinetics between CO₂ and alkanolamines both in aqueous and non-aqueous solutions. An overview. *Chem. Eng. Commun.* 144, 113–158.
- Walker, R.C., Crowley, M.F., Case, D.A., 2008. The implementation of a fast and accurate QM/MM potential method in Amber. *J. Comput. Chem.* 29, 1019–1031.
- Wang, J., Wolf, R.M., Caldwell, J.W., Kollman, P.A., Case, D.A., 2004. Development and testing of a general amber force field. *J. Comput. Chem.* 25, 1157–1174.
- Xie, H.B., Zhou, Y.Z., Zhang, Y.K., Johnson, J.K., 2010. Reaction mechanism of monoethanolamine with CO₂ in aqueous solution from molecular modeling. *J. Phys. Chem. A* 114, 11844–11852.
- Xie, H.-B., He, N., Song, Z., Chen, J., Li, X., 2014. Theoretical investigation on the different reaction mechanisms of aqueous 2-amino-2-methyl-1-propanol and monoethanolamine with CO₂. *Ind. Eng. Chem. Res.* 53, 3363–3372.
- Yamada, H., 2016. Comparison of solvation effects on CO₂ capture with aqueous amine solutions and amine-functionalized ionic liquids. *J. Phys. Chem. B* 120, 10563–10568.
- Yang, Q., Puxty, G., James, S., Bown, M., Feron, P., Conway, W., 2016. Toward intelligent CO₂ capture solvent design through experimental solvent development and amine synthesis. *Energy Fuels* 30, 7503–7510.
- Yang, X., Rees, R.J., Conway, W., Puxty, G., Yang, Q., Winkler, D.A., 2017. Computational modeling and simulation of CO₂ capture by aqueous amines. *Chem. Rev.* 117, 9524–9593.
- Yu, C.-H., Huang, C.-H., Tan, C.-S., 2012. A review of CO₂ capture by absorption and adsorption. *Aerosol Air Qual. Res.* 12, 745–769.
- Yu, J., Xie, L.H., Li, J.R., Ma, Y., Seminario, J.M., Balbuena, P.B., 2017. CO₂ capture and separations using MOFs: computational and experimental studies. *Chem. Rev.* 117, 9674–9754.
- Yuan, Y., Rochelle, G.T., 2019. Lost work: A comparison of water-lean solvent to a second generation aqueous amine process for CO₂ capture. *Int. J. Greenh. Gas Con.* 84, 82–90.
- Zhang, T., Yu, Y., Zhang, Z., 2018. Effects of non-aqueous solvents on CO₂ absorption in monoethanolamine: ab initio calculations. *Mol. Simul.* 44, 815–825.
- Zhong, N., Liu, H., Luo, X., Al-Marri, M.J., Benamor, A., Idem, R., et al., 2016. Reaction kinetics of carbon dioxide (CO₂) with diethylenetriamine and 1-amino-2-propanol in nonaqueous solvents using stopped-flow technique. *Ind. Eng. Chem. Res.* 55, 7307–7317.
- Zielkiewicz, J., 2005. Structural properties of water: comparison of the SPC, SPCE, TIP4P, and TIP5P models of water. *J. Chem. Phys.* 123, 104501.